

## Designing Linear Amplifiers Using the IL300 Optocoupler Appnote 50

by Bob Krause

### Introduction

This application note presents isolation amplifier circuit designs useful in industrial, instrumentation, medical, and communication systems. It covers the IL300's coupling specifications, and circuit topologies for photovoltaic and photoconductive amplifier design. Specific designs include unipolar and bipolar responding amplifiers. Both single ended and differential amplifier configurations are discussed. Also included is a brief tutorial on the operation of photodetectors and their characteristics.

Galvanic isolation is desirable and often essential in many measurement systems. Applications requiring galvanic isolation include: industrial sensors, medical transducers, and mains powered switch mode power supplies. Operator safety and signal quality are insured with isolated interconnections. These isolated interconnections commonly use isolation amplifiers.

Industrial sensors include thermocouples, strain gauges, and pressure transducers. They provide monitoring signals to a process control system. Their low level DC and AC signal must be accurately measured in the presence of high common mode noise. The IL300's 130 dB common mode rejection (CMR),  $\pm 50$  ppm/ $^{\circ}$ C stability and  $\pm 0.01\%$  linearity provide a quality link from the sensor to the controller input.

Safety is an important factor in instrumentation for medical patient monitoring. EEG, ECG, and similar systems demand high insulation safety for the patient under evaluation. The IL300's 7500 V Withstand Test Voltage (WTV) insulation, DC response, and high CMR are features which assure safety for the patient and accuracy of the transducer signals.

The aforementioned applications require isolated signal processing. Current designs rely on A to D or V to F converters to provide input/output insulation and noise isolation. Such designs use transformers or high speed optocouplers which often result in complicated and costly solutions. The IL300 eliminates the complexity of these isolated amplifier designs without sacrificing accuracy or stability.

The IL300's 200 KHz bandwidth and gain stability make it an excellent candidate for subscriber and data phone interfaces.

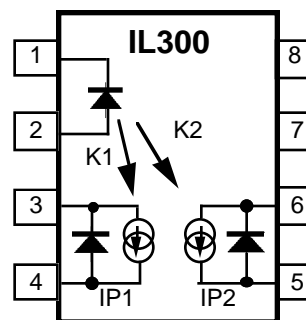
Present OEM switch mode power supplies are approaching 1 MHz switching frequencies. Such supplies need output monitoring feedback networks with wide bandwidth and flat phase response. The IL300 satisfies these needs with simple support circuits.

### Operation of the IL300

The IL300 consists of a high efficiency AlGaAs LED emitter coupled to two independent PIN photodiodes. The servo (pins 3, 4) photodiode provides a feedback signal which controls the current to the LED emitter (pins 1, 2). This photodiode provides a photocurrent,  $I_{p1}$ , that is directly proportional to the LED's incident flux. This servo operation linearizes the LED's output flux and eliminates the LED's time and temperature. The galvanic isolation between the input and the output is provided by a second PIN photodiode (pins 5, 6) located on the output side of the coupler. The output current,  $I_{p2}$ , from this photodiode accurately tracks the photocurrent generated by the servo photodiode.

Figure 1 shows the package footprint and electrical schematic of the IL300. The following sections discuss the key operating characteristics of the IL300. The IL300 performance characteristics are specified with the photodiodes operating in the photoconductive mode.

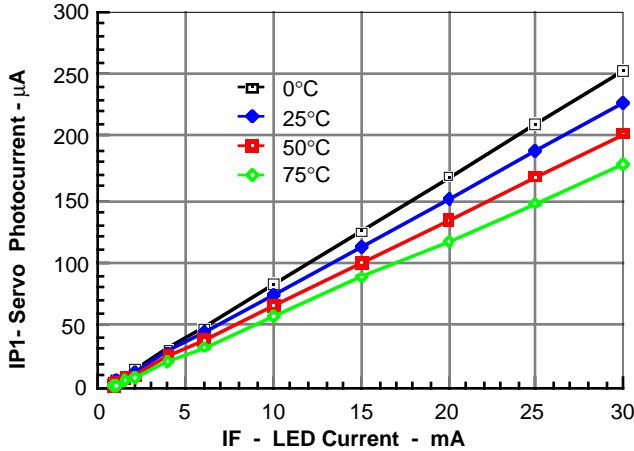
Figure 1. IL300 schematic



## Servo Gain—K1

The typical servo photocurrent,  $I_{P1}$ , as a function of LED current, is shown in Figure 2. This graph shows the typical nonservo LED-photodiode linearity is  $\pm 1\%$  over an LED drive current range of 1 to 30 mA. This curve also shows that the nonservo photocurrent is affected by ambient temperature. The photocurrent typically decreases by  $-0.5\%$  per  $^{\circ}\text{C}$ . The LED's nonlinearity and temperature characteristics are minimized when the IL300 is used as a servo linear amplifier.

**Figure 2. Servo photocurrent vs. LED current**



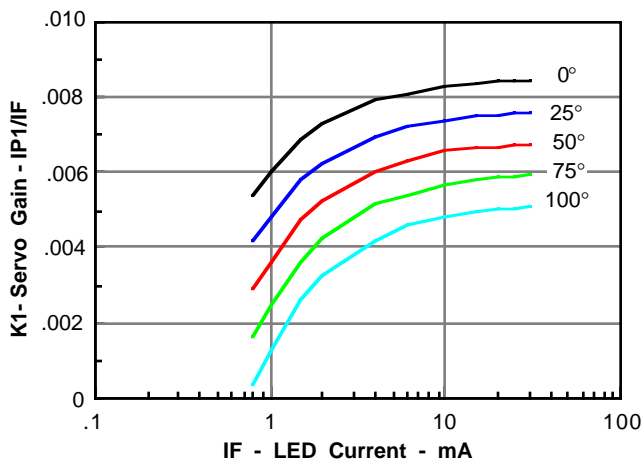
The servo gain is defined as the ratio of the servo photocurrent,  $I_{P1}$ , to the LED drive current,  $I_F$ . It is called K1, and is described in Equation 1.

$$\text{Equation 1: } K1 = I_{P1} / I_F$$

The IL300 is specified with an  $I_F = 10 \text{ mA}$ ,  $T_A = 25^{\circ}\text{C}$ , and

$V_d = -15 \text{ V}$ . This condition generates a typical servo photocurrent of  $I_{P1} = 70 \mu\text{A}$ . This results in a typical  $K1 = 0.007$ . The relationship of K1 and LED drive current is shown in Figure 3.

**Figure 3. Servo gain vs. LED current**



The servo gain, K1, is guaranteed to be between 0.005 minimum to 0.011 maximum of an  $I_F = 10 \text{ mA}$ ,  $T_A = 25^{\circ}\text{C}$ , and  $V_D = -15 \text{ V}$ .

**Figure 4. Normalized servo gain vs. LED current**

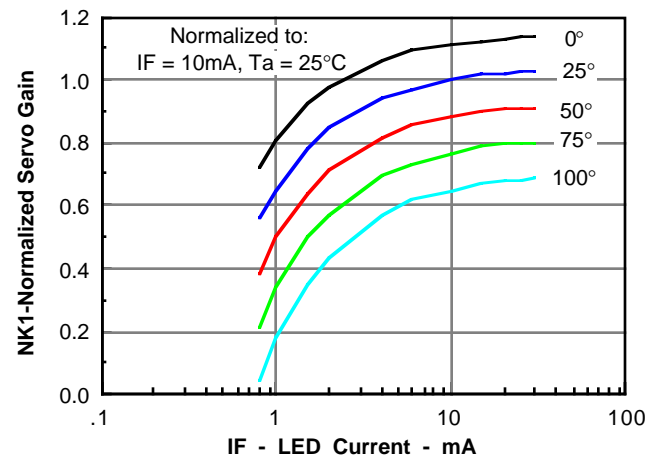


Figure 4 presents the Normalized servo gain,  $NK1(I_F, T_A)$ , as a function of LED current and temperature. It can be used to determine the minimum or maximum servo photocurrent,  $I_{P1}$ , given LED current and ambient temperature. The actual servo gain can be determined from equation 2.

$$\text{Equation 2: } K1(I_F, T_A) = K1(\text{data sheet limit}) \cdot NK1(I_F, T_A)$$

The minimum servo photocurrent under specific use conditions can be determined by using the minimum value for K1 (0.005) and the normalization factor from Figure 4. The example is to determine  $I_{P1}(\text{min})$  for the condition of K1 at  $T_A = 75^{\circ}\text{C}$ , and  $I_F = 6 \text{ mA}$ .

$$\text{Equation 3: } NK1(I_F = 6 \text{ mA}, T_A = 75^{\circ}\text{C}) = 0.72 \cdot NK1(I_F, T_A)$$

$$\text{Equation 4: } K1 \text{ MIN}(I_F, T_A) = K1 \text{ MIN}(0.005) \cdot NK1(0.72)$$

$$\text{Equation 5: } K1 \text{ MIN}(I_F, T_A) = 0.0036$$

Using  $K1(I_F, T_A) = 0.0036$  in Equation 1 the minimum  $I_{P1}$  can be determined.

$$\text{Equation 6: } I_{P1} \text{ MIN} = K1 \text{ MIN}(I_F, T_A) \cdot I_F$$

$$\text{Equation 7: } I_{P1} \text{ MIN} = 0.0036 \cdot 6 \text{ mA}$$

$$\text{Equation 8: } I_{P1} \text{ MIN}(I_F = 6 \text{ mA}, T_A = 75^{\circ}\text{C}) = 21.6 \mu\text{A}$$

The minimum value  $I_{P1}$  is useful for determining the maximum required LED current needed to servo the input stage of the isolation amplifier.

## Output Forward Gain—K2

Figure 1 shows that the LED's optical flux is also received by a PIN photodiode located on the output side (pins 5, 6) of the coupler package. This detector is surrounded by an optically transparent high voltage insulation material. The coupler construction spaces the LED 0.4 mm from the output PIN photodiode. The package construction and the insulation material guarantee the coupler to have a Withstand Test Voltage of 7500 V peak.

K2, the output (forward) gain is defined as the ratio of the output photodiode current,  $I_{P2}$ , to the LED current,  $I_F$ . K2 is shown in Equation 9.

$$\text{Equation 9: } K2 = I_{P2} / I_F$$

The forward gain,  $K_2$ , has the same characteristics of the servo gain,  $K_1$ . The normalized current and temperature performance of each detector is identical. This results from using matched PIN photodiodes in the IL300's construction.

### Transfer Gain – $K_3$

The current gain, or CTR, of the standard phototransistor optocoupler is set by the LED efficiency, transistor gain, and optical coupling. Variation in ambient temperature alters the LED efficiency and phototransistor gain and result in CTR drift. Isolation amplifiers constructed with standard phototransistor optocouplers suffer from gain drift due to changing CTR.

Isolation amplifiers using the IL300 are not plagued with the drift problems associated with standard phototransistors. The following analysis will show how the servo operation of the IL300 eliminates the influence of LED efficiency on the amplifier gain.

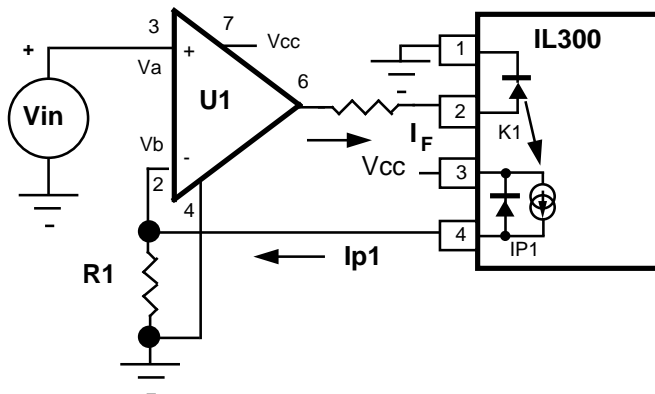
The input-output gain of the IL300 is termed transfer gain,  $K_3$ . Transfer gain is defined as the output (forward) gain,  $K_2$ , divided by servo gain,  $K_1$ , as shown in Equation 10.

$$\text{Equation 10: } K_3 = K_2 / K_1$$

The first step in the analysis is to review the simple optical servo feedback amplifier shown in Figure 5.

The circuit consists of an operational amplifier,  $U_1$ , a feedback resistor  $R_1$ , and the input section of the IL300. The servo photodiode is operating in the photoconductive mode. The initial conditions are:  $V_a = V_b = 0$  V. Initially, a positive voltage is applied to the noninverting input ( $V_a$ ) of the opamp. At that time the output of the opamp will swing toward the positive  $V_{cc}$  rail, and forward bias the LED. As the LED current,  $I_F$ , starts to flow, an optical flux will be generated. The optical flux will irradiate the servo photodiode causing it to generate a photocurrent,  $I_{p1}$ . This photocurrent will flow through  $R_1$  and develop a positive voltage at the inverting input ( $V_b$ ) of the operational amplifier. The amplifier output will start to swing toward the negative supply rail,  $-V_{cc}$ . When the magnitude of the  $V_b$  is equal to that of  $V_a$ , the LED drive current will cease to increase. This condition forces the circuit into a stable closed loop condition.

**Figure 5. Optical servo amplifier**



When  $V_{in}$  is modulated,  $V_b$  will track  $V_{in}$ . For this to happen the photocurrent through  $R_1$  must also track the change in  $V_a$ . Recall that the photocurrent results from the change in LED current times the servo gain,  $K_1$ . The following equations can be written to describe this activity.

$$\text{Equation 11: } V_a = V_b = V_{in} = 0$$

$$\text{Equation 12: } I_{p1} = I_F \cdot K_1$$

$$\text{Equation 13: } V_b = I_{p1} \cdot R_1$$

The relationship of LED drive to input voltage is shown by combining Equations 11, 12, and 13.

$$\text{Equation 14: } V_a = I_{p1} \cdot R_1$$

$$\text{Equation 15: } V_{in} = I_F \cdot K_1 \cdot R_1$$

$$\text{Equation 16: } I_F = V_{in} / (K_1 \cdot R_1)$$

Equation 16 shows that the LED current is related to the input voltage  $V_{in}$ . A changing  $V_a$  causes a modulation in the LED flux. The LED flux will change to a level that generates the necessary servo photocurrent to stabilize the optical feedback loop. The LED flux will be a linear representation of the input voltage,  $V_a$ . The servo photodiode's linearity controls the linearity of the isolation amplifier.

The next step in the analysis is to evaluate the output transresistance amplifier. The common inverting transresistance amplifier is shown in Figure 6. The output photodiode is operated in the photoconductive mode. The photocurrent,  $I_{p2}$ , is derived from the same LED that irradiates the servo photodiode. The output signal,  $V_{out}$ , is proportional to the output photocurrent,  $I_{p2}$ , times the transresistance,  $R_2$ .

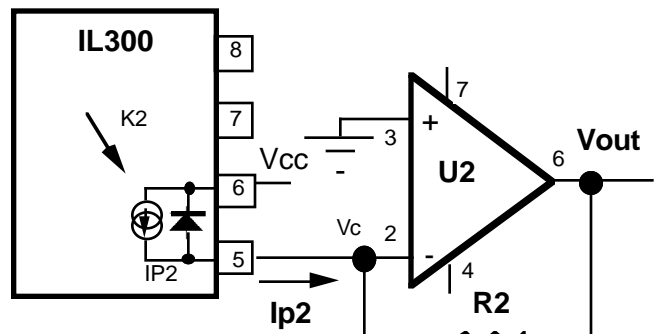
$$\text{Equation 17: } V_{out} = -I_{p2} \cdot R_2$$

$$\text{Equation 18: } I_{p2} = K_2 \cdot I_F$$

Combining Equations 17 and 18 and solving for  $I_F$  is shown in Equation 19.

$$\text{Equation 19: } I_F = -V_{out} / (K_2 \cdot R_2)$$

**Figure 6. Output transresistance amplifier**



The input-output gain of the isolation amplifier is determined by combining Equations 16 and 19.

Equation 16:  $I_F = V_{in} / (K_1 \cdot R_1)$

Equation 19:  $I_F = -V_{out} / (K_2 \cdot R_2)$

Equation 20:  $V_{in} / (K_1 \cdot R_1) = -V_{out} / (K_2 \cdot R_2)$

Equation 21 gives the solution for the input-output gain.

Equation 21:  $V_{out} / V_{in} = -(K_2 \cdot R_2) / (K_1 \cdot R_1)$

Note that the LED current,  $I_F$ , is factored out of Equation 21. This is possible because the servo and output photodiode currents are generated by the same LED source. This equation can be simplified further by replacing the  $K_2/K_1$  ratio with IL300's transfer gain,  $K_3$ .

Equation 22:  $V_{out} / V_{in} = -K_3 \cdot (R_2 / R_1)$

The IL300 isolation amplifier gain stability and offset drift depends on the transfer gain characteristics. Figure 7 shows the consistency of the normalized  $K_3$  as a function of LED current and ambient temperature. The transfer gain drift as a function of temperature is  $\pm 0.005\%/^{\circ}\text{C}$  over a  $0^{\circ}\text{C}$  to  $75^{\circ}\text{C}$  range.

Figure 8 shows the composite isolation amplifier including the input servo amplifier and the output transresistance amplifier. This circuit offers the insulation of an optocoupler and the gain stability of a feedback amplifier.

Figure 7. Normalized servo transfer gain

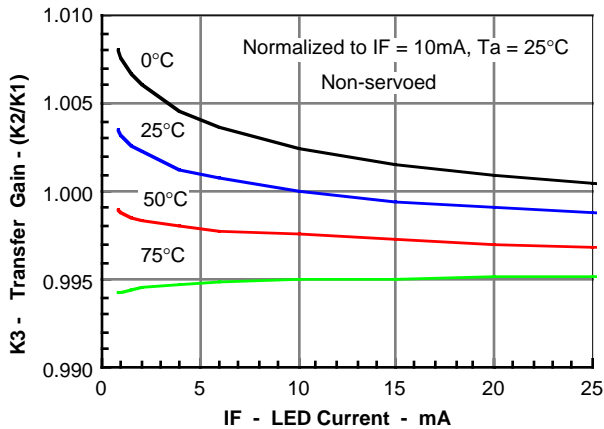
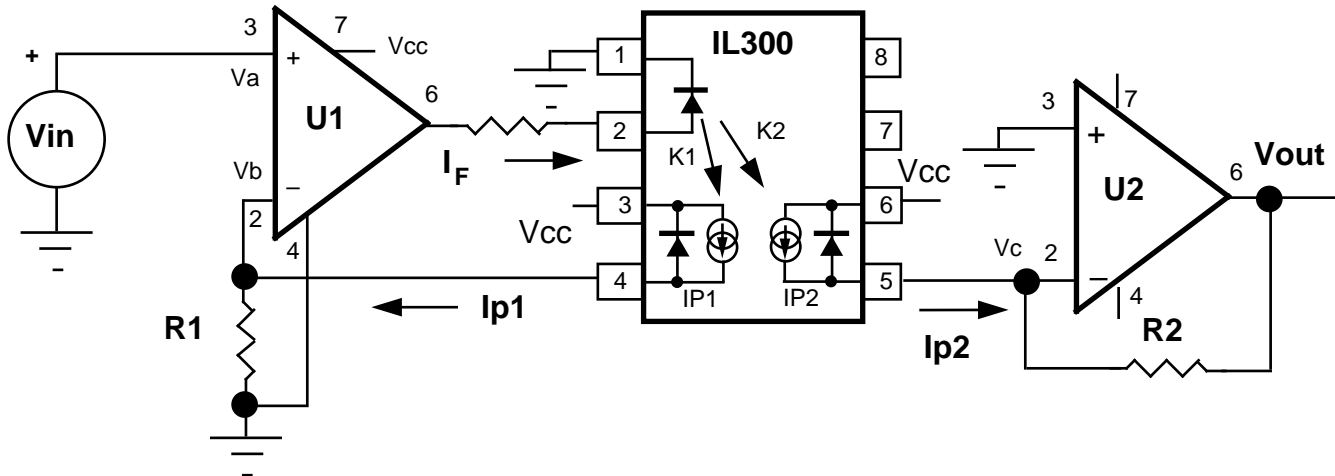


Figure 8. Composite amplifier



An instrumentation engineer often seeks to design an isolation amplifier with unity gain:  $V_{out} / V_{in} = 1.0$ . The IL300's transfer gain is targeted for unity gain:  $K_3 = 1.0$ . Package assembly variations result in a range of  $K_3$ . Because of the importance of  $K_3$ , Siemens offers the transfer gain sorted into  $\pm 5\%$  bins. The bin designator is listed on the IL300 package. The  $K_3$  bin limits are shown in Table 1.

This table is useful when selecting the specific resistor values needed to set the isolation amplifier transfer gain.

Table 1.  $K_3$  Transfer Gain Bins

BIN	Typ.	Min.	Max.
A	0.59	0.56	0.623
B	0.66	0.623	0.693
C	0.73	0.693	0.769
D	0.81	0.769	0.855
E	0.93	0.855	0.95
F	1.0	0.95	1.056
G	1.11	1.056	1.175
H	1.24	1.175	1.304
I	1.37	1.304	1.449
J	1.53	1.449	1/61

### Isolation Amplifier Design Techniques

The previous section discussed the operation of an isolation amplifier using the optical servo technique. The following section will describe the design philosophy used in developing isolation amplifiers optimized for input voltage range, linearity, and noise rejection.

The IL300 can be configured as either a photovoltaic or photoconductive isolation amplifier. The photovoltaic topology offers the best linearity, lowest noise, and drift performance. Isolation amplifiers using these circuit configurations meet or exceed 12 bit AD performance. Photoconductive photodiode operation provides the largest coupled frequency bandwidth. The photoconductive configuration has linearity and drift characteristics comparable to a 8-9 bit AD converter.

## Photovoltaic Isolation Amplifier

The transfer characteristics of this amplifier are shown in Figure 9.

When low offset drift and greater than 12 bit linearity is desired, photovoltaic amplifier designs should be considered. The schematic of a typical positive unipolar photovoltaic isolation amplifier is shown in Figure 10.

The input stage consists of a servo amplifier, U1, which controls the LED drive current. The servo photodiode is operated with zero voltage bias. This is accomplished by connecting the photodiodes anode and cathode directly to U1's inverting and non-inverting inputs. The characteristics of the servo amplifier operation are presented in Figure 10a and Figure 10b. The servo photocurrent is linearly proportional to the input voltage,  $I_{P1} = V_{IN}/R1$ . Figure 10b shows the LED current is inversely proportional to the servo transfer gain,  $I_F = I_{P1}/K1$ . The servo photocurrent, resulting from the LED emission, keeps the voltage at the inverting input of U1 equal to zero. The output photocurrent,  $I_{P2}$ , results from the incident flux supplied by the LED. Figure 10c shows that the magnitude of the output current is determined by the output transfer gain,  $K2$ . The output voltage, as shown in Figure 10d, is proportional to the output photocurrent  $I_{P2}$ . The output voltage equals the product of the output photocurrent times the output amplifier's transresistance,  $R2$ .

The composite amplifier transfer gain ( $V_o/V_{in}$ ) is the ratio of two products. The first is the output transfer gain,  $K2 \cdot R2$ .

**Figure 9. Positive unipolar photovoltaic isolation amplifier transfer characteristics**

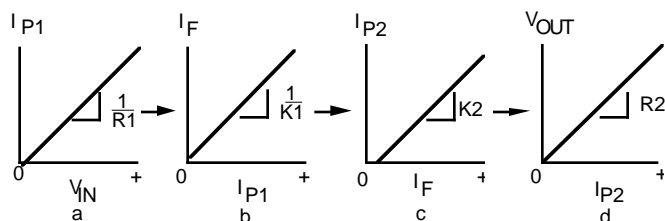
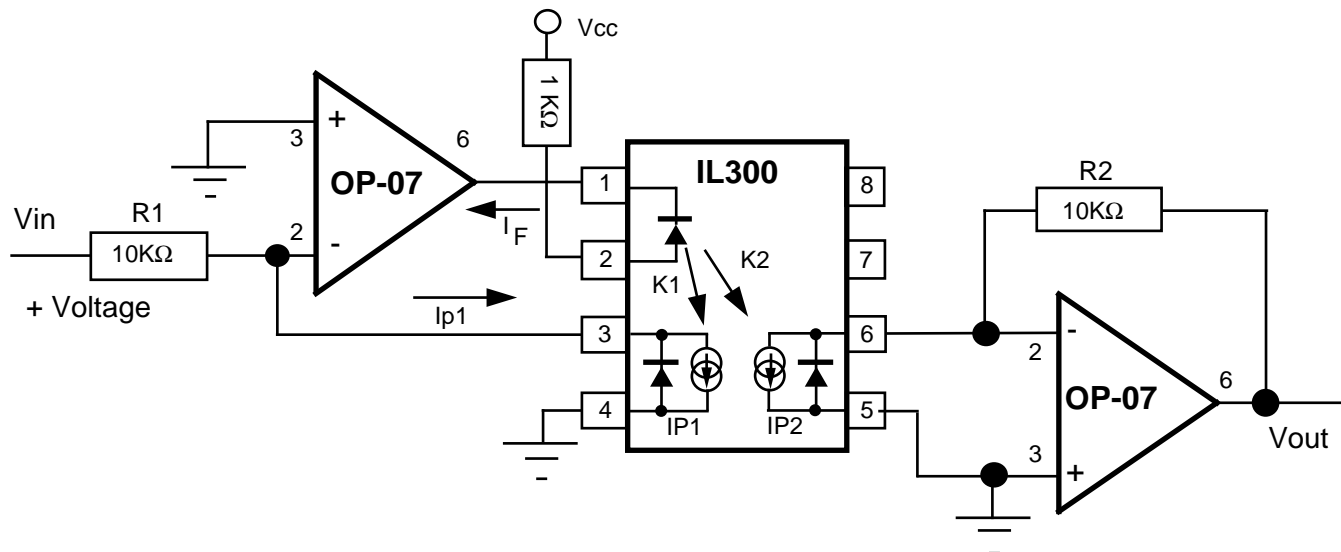


**Figure 10. Positive unipolar photovoltaic amplifier**



The second is the servo transfer gain,  $K1 \cdot R1$ . The amplifier gain is the first divided by the second. See Equation 23.

Equation 23:

$$\frac{V_o}{V_{in}} = \frac{K2 \cdot R2}{K1 \cdot R1}$$

Equation 23 shows that the composite amplifier transfer gain is independent of the LED forward current. The  $K2/K1$  ratio reduces to IL300 transfer gain,  $K3$ . This relationship is included in Equation 24. This equation shows that the composite amplifier gain is equal to the product of the IL300 gain,  $K3$ , times the ratio of the output to input resistors.

Equation 24:

$$\frac{V_o}{V_o} = \frac{K3 \cdot R2}{R1}$$

Designing this amplifier is a three step process. First, given the input signal span and U1's output current handling capability, the input resistor  $R1$  can be determined by using the circuit found in Figure 9 and the following typical characteristics:

OP-07	$I_{out} = \pm 15 \text{ mA}$
IL300	$K1 = 0.007$
	$K2 = 0.007$
	$K3 = 1.0$
$V_{in}$	$0 \geq + 1.0 \text{ V}$

The second step is to determine servo photocurrent,  $I_{P1}$ , resulting from the peak input signal swing. This current is the product of the LED drive current,  $I_F$  times the servo transfer gain,  $K1$ . For this example the  $I_{outmax}$  is equal to the largest LED current signal swing, i.e.,  $I_F = I_{outmax}$ .

$$I_{P1} = K1 \cdot I_{outmax}$$

$$I_{P1} = 0.007 \cdot 15 \text{ mA}$$

$$I_{P1} = 105 \mu\text{A}$$

The input resistor, R1, is set by the input voltage range and the peak servo photocurrent,  $I_{p1}$ . Thus R1 is equal to:

$$R1 = V_{in} / I_{p1}$$

$$R1 = 1.0 / 105 \mu A$$

$$R1 = 9.524 K\Omega$$

R1 is rounded to 10 K $\Omega$ .

The third step in this design is determining the value of the trans resistance, R2, of the output amplifier. R2 is set by the composite voltage gain desired, and the IL300's transfer gain, K3.

Given  $K3 = 1.0$  and a required  $V_{out}/V_{in} = G = 1.0$ , the value of R2 can be determined.

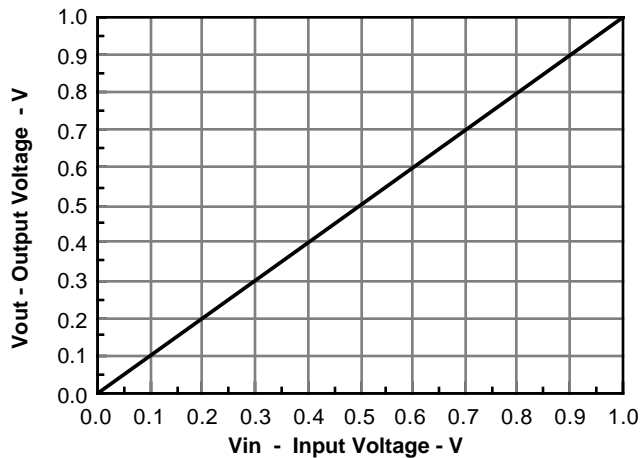
$$R2 = (R1 \cdot G) / K3$$

$$R2 = (10 K\Omega \cdot 1.0) / 1.0$$

$$R2 = 10 K\Omega$$

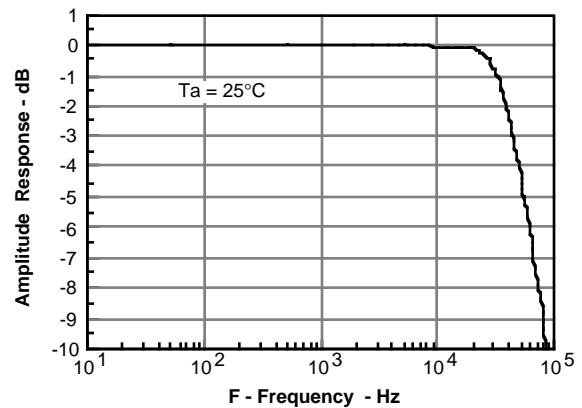
When the amplifier in Figure 9 is constructed with OP-07 operational amplifiers it will have the characteristics shown in Figure 11 and Figure 12.

**Figure 11. Photovoltaic amplifier transfer gain**



The frequency response is shown in Figure 12. This amplifier has a small signal bandwidth of 45 KHz.

**Figure 12. Photovoltaic amplifier frequency response**



The amplifier in Figure 9 responds to positive polarity input signals. This circuit can be modified to respond to negative polarity signals. The modifications of the input amplifier include reversing the polarity of the servo photodiode at U1's input and connecting the LED so that it sinks current from U1's output. The noninverting isolation amplifier response is maintained by reversing the IL300's output photodiodes connection to the input of the transresistance amplifier. The modified circuit is shown in Figure 13.

The negative unipolar photovoltaic isolation amplifier transfer characteristics are shown in Figure 14. This amplifier, as shown in Figure 13, responds to signals in only one quadrant. If a positive signal is applied to the input of this amplifier, it will forward bias the photodiode, causing U1 to reverse bias the LED. No damage will occur, and the amplifier will be cut off under this condition. This operation is verified by the transfer characteristics shown in Figure 14.

**Figure 13. Negative unipolar photovoltaic isolation amplifier**

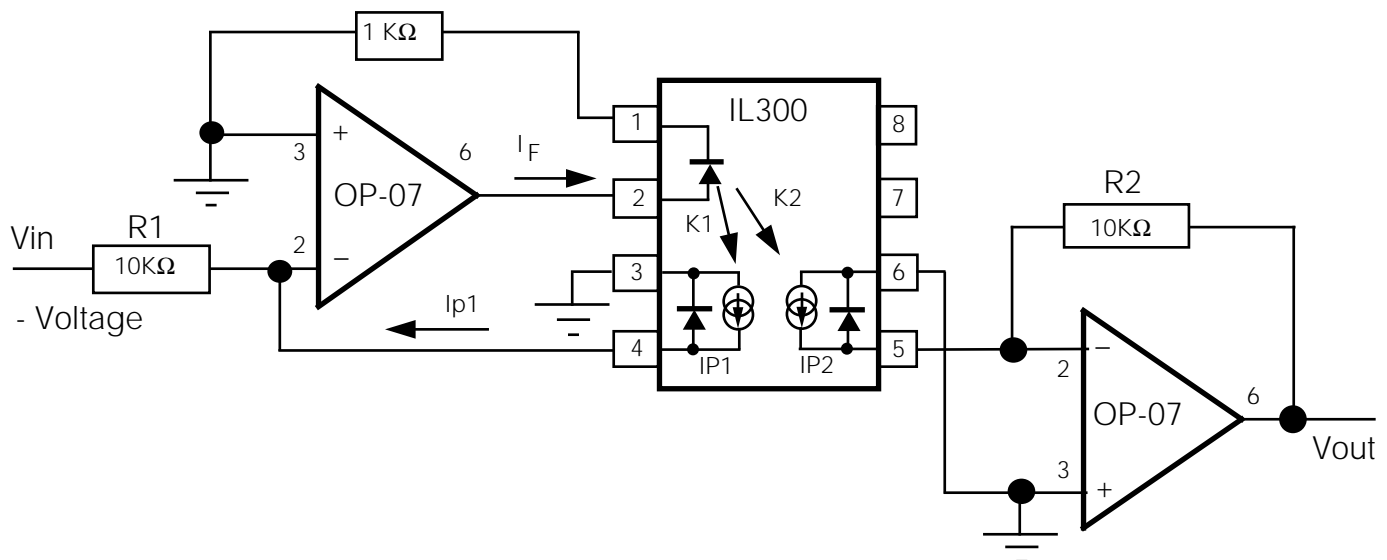
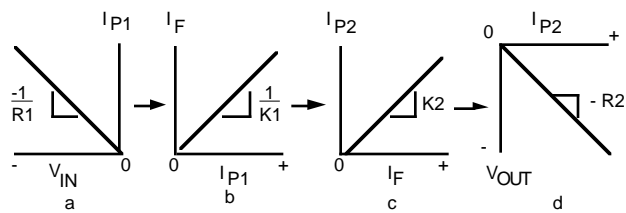


**Figure 14. Negative unipolar photovoltaic isolation amplifier transfer characteristics**



A bipolar responding photovoltaic amplifier can be constructed by combining a positive and negative unipolar amplifier into one circuit. This is shown in Figure 15. This amplifier uses two IL300s with each detector and LED connected in antiparallel. The IL300a responds to positive signals while the IL300b is active for the negative signals. The operation of the IL300s and the U1 and U2 is shown in the transfer characteristics given in Figure 16.

**Figure 15. Bipolar input photovoltaic isolation amplifier**

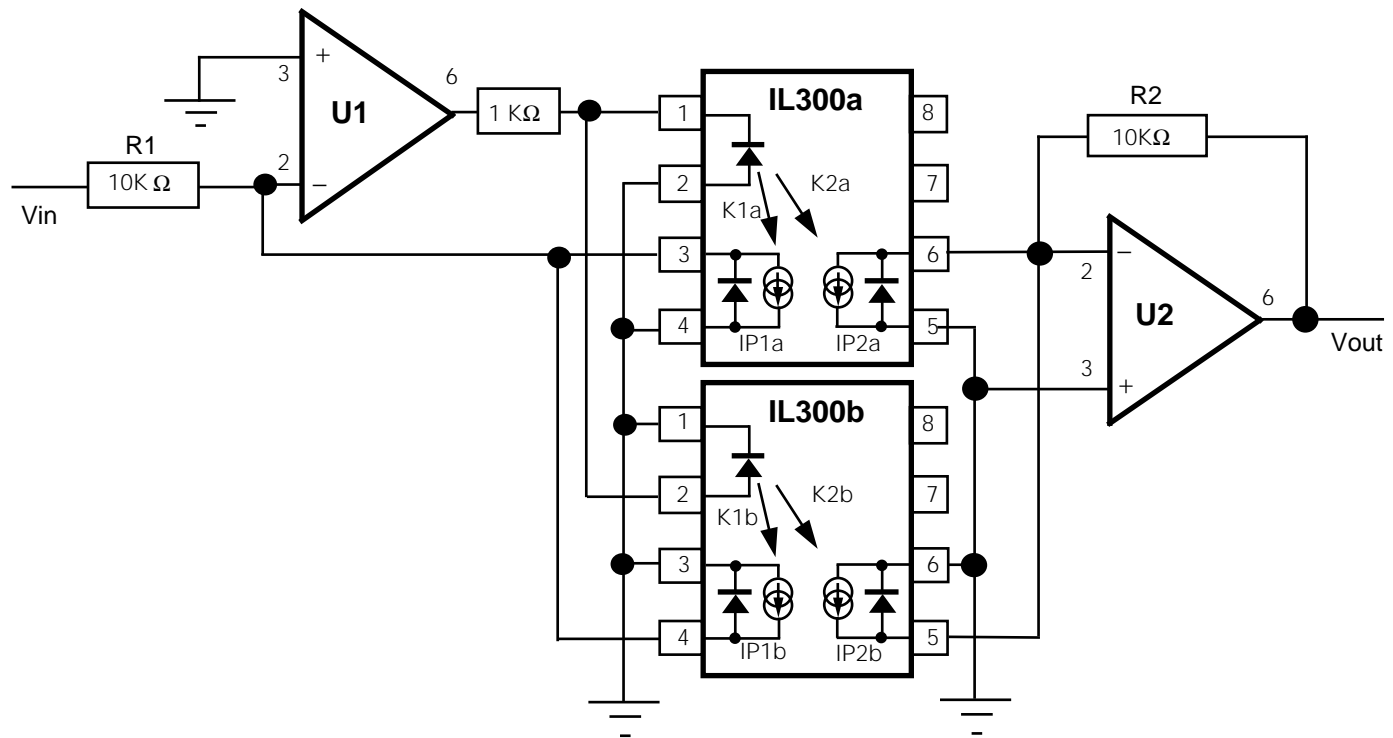
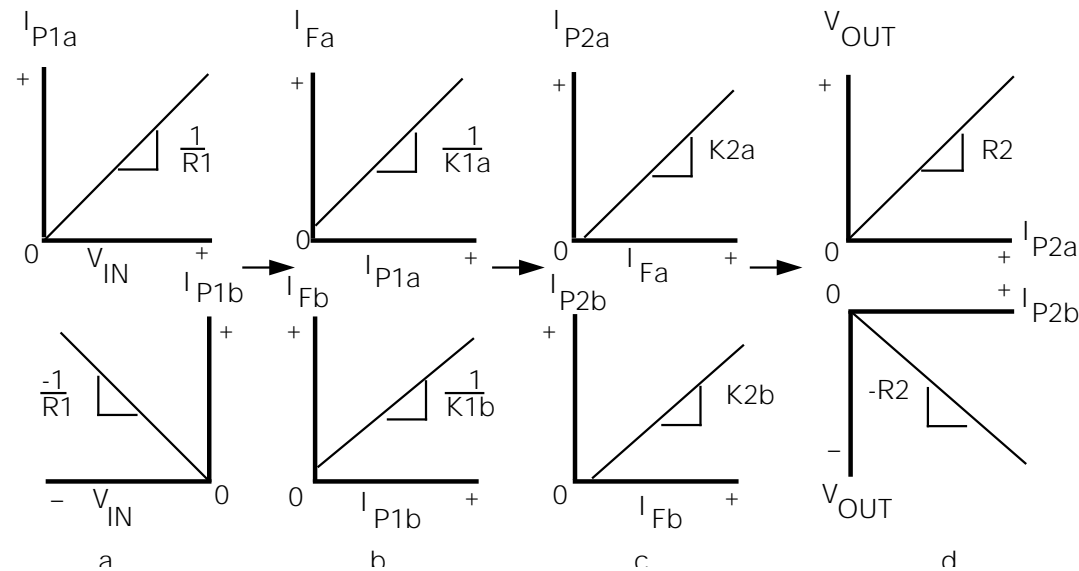


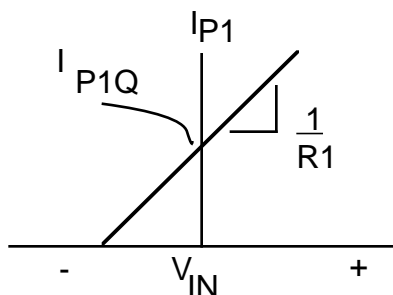
**Figure 16. Bipolar input photovoltaic isolation amplifier transfer characteristics**



The operational analysis of this amplifier is similar to the positive and negative unipolar isolation amplifier. This simple circuit provides a very low offset drift and exceedingly good linearity. The circuit's useful bandwidth is limited by crossover distortion resulting from the photodiode stored charge. With a bipolar signal referenced to ground and using a 5% distortion limit, the typical bandwidth is under 1 KHz. Using matched K3s, the composite amplifier gain for positive and negative voltage will be equal.

Whenever the need to couple bipolar signals arises a pre-biased photovoltaic isolation amplifier is a good solution. By pre-biasing the input amplifier the LED and photodetector will operate from a selected quiescent operating point. The relationship between the servo photocurrent and the input voltage is shown in Figure 17.

**Figure 17. Transfer characteristic prebiased photovoltaic bipolar amplifier**



The quiescent operation point,  $I_{P1Q}$ , is determined by the dynamic range of the input signal. This establishes maximum LED current requirements. The output current capability of the OP-07 is extended by including a buffer transistor between the output of U1 and the LED. The buffer transistor minimizes thermal drift by reducing the OP-07 internal power dissipation if it were to drive the LED directly. This is shown in Figure 18.

The bias is introduced into the inverting input of the servoamplifier, U1. The bias forces the LED to provide photocurrent,  $I_{P1}$ , to servo the input back to a zero volt equilibrium. The bias source can be as simple as a series resistor connected to  $V_{CC}$ . Best stability and minimum offset drift is achieved when a good quality current source is used. Figure 20 shows the amplifier found in Figure 18 including two modified Howland current sources. The first source prebiases the servo amplifier, and the second source is connected to U2's inverting input which matches the input prebias.

**Figure 19. Prebiased photovoltaic isolation amplifier transfer characteristics**

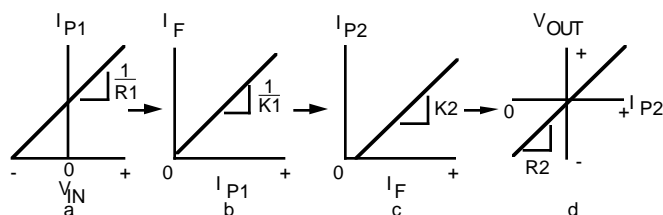


**Figure 18. Prebiased photovoltaic isolation amplifier**

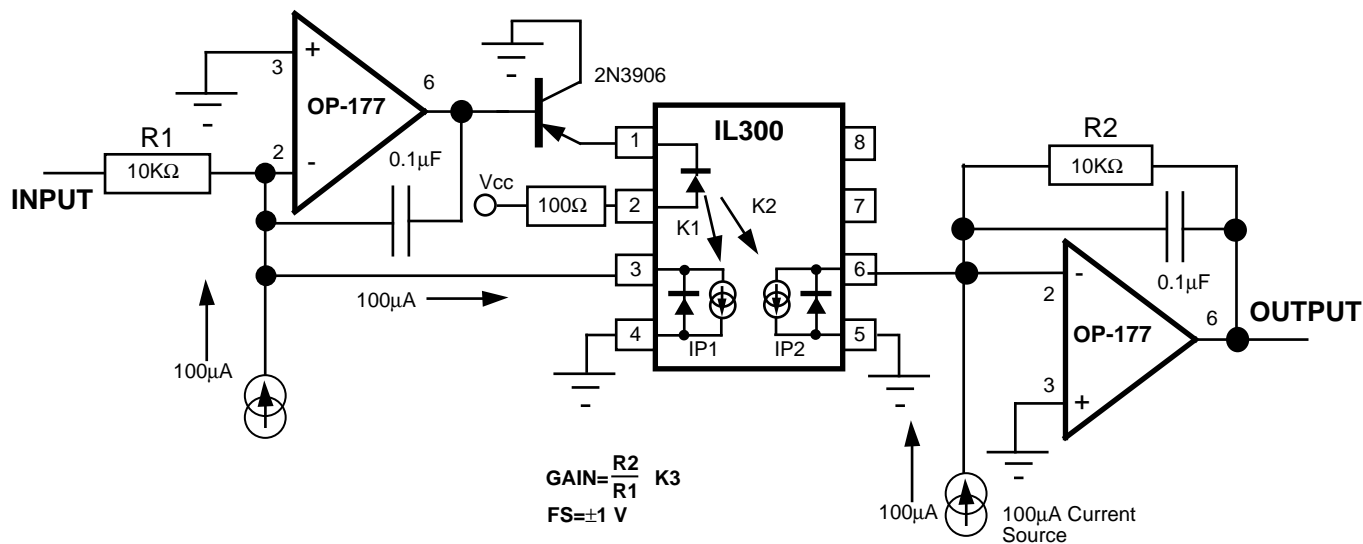




Figure 20. Prebiased photovoltaic isolation amplifier

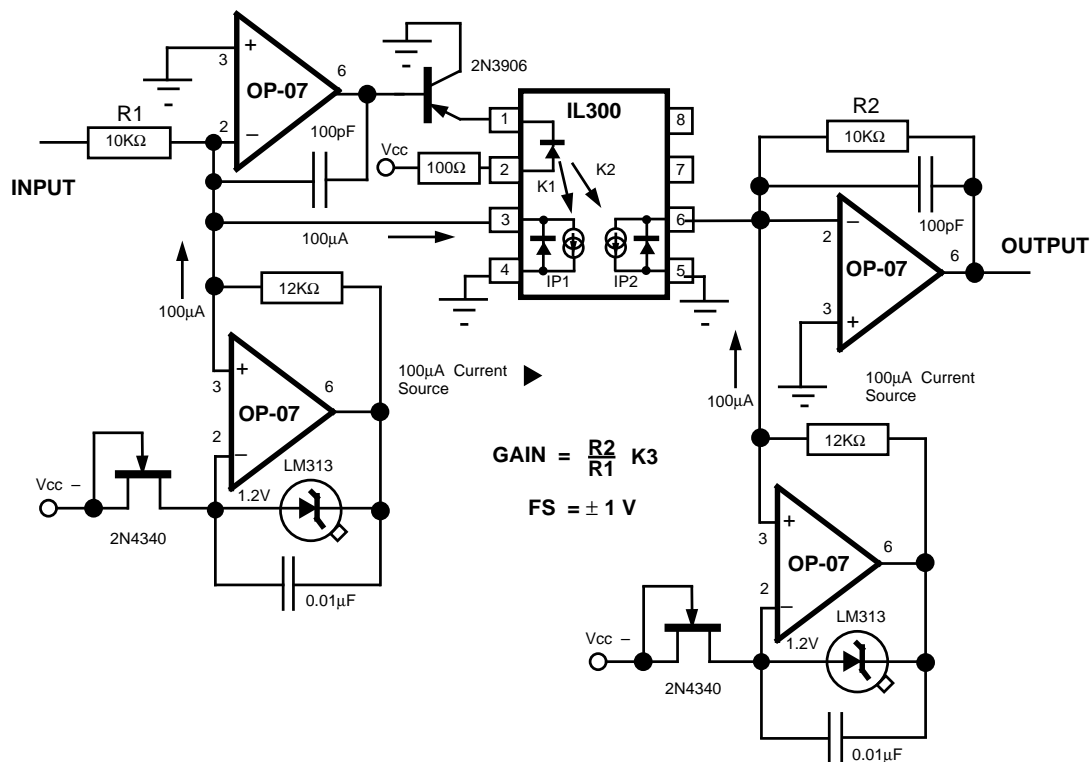
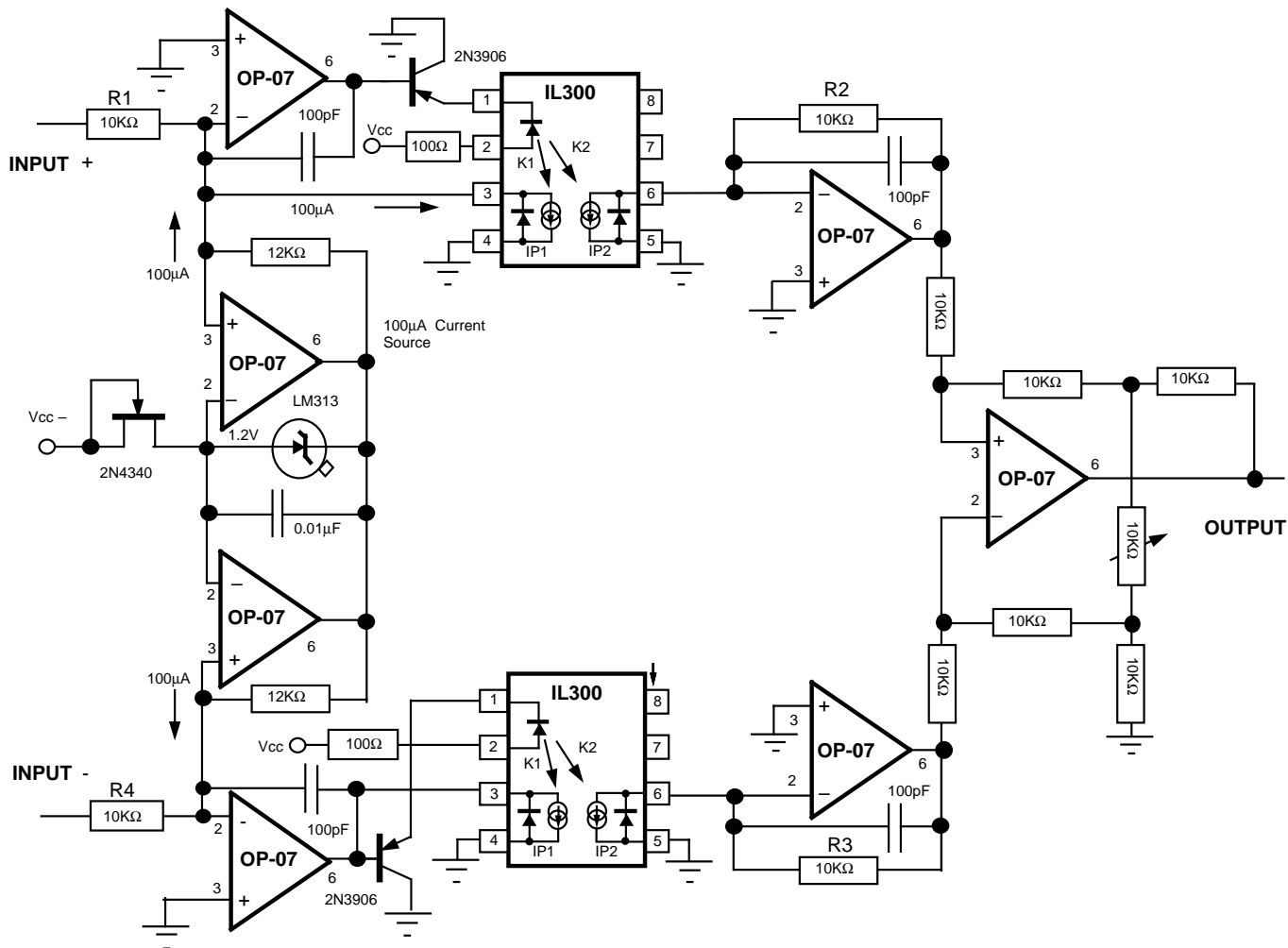


Figure 21. Differential prebiased photovoltaic isolation amplifier



The previous circuit offers a DC/AC coupled bipolar isolation amplifier. The output will be zero volts for an input of zero volts. This circuit exhibits exceptional stability and linearity. This circuit has demonstrated compatibility with 12 bit A/D converter systems. The circuit's common mode rejection is determined by CMR of the IL300. When higher common mode rejection is desired one can consider the differential amplifier shown in Figure 21.

This amplifier is more complex than the circuit shown in Figure 20. The complexity adds a number of advantages. First the CMR of this isolation amplifier is the product of the IL300 and that of the summing differential amplifier found in the output section. Note also that the need for an offsetting bias source at the output is no longer needed. This is due to differential configuration of the two IL300 couplers. This amplifier is also compatible with instrumentation amplifier designs. It offers a bandwidth of 50KHz, and an extremely good CMR of 140dB at 10 KHz.

### Photoconductive Isolation Amplifier

The photoconductive isolation amplifier operates the photodiodes with a reverse bias. The operation of the input network is covered in the discussion of K3 and as such will not be repeated here. The photoconductive isolation amplifier is recommended when maximum signal bandwidth is desired.

### Unipolar Isolation Amplifier

The circuit shown in Figure 22 is a unipolar photoconductive amplifier and responds to positive input signals. The gain of this amplifier follows the familiar form of  $V_o/V_{in} = G = K3 \cdot (R2 / R1)$ . R1 sets the input signal range in conjunction with the servo gain and the maximum output current,  $I_o$ , which U1 can source. Given this,  $I_{o_{max}} = I_{F_{max}}$ . R1 can be determined from Equation 28.

$$\text{Equation 28: } R1 = V_{in_{max}} / (K1 \cdot I_{o_{max}})$$

The output section of the amplifier is a voltage follower. The output voltage is equal to the voltage created by the output photocurrent times the photodiode load resistor, R2. This resistor is used to set the composite gain of the amplifier as shown in Equation 29.

$$\text{Equation 29: } R2 = (R1 \cdot G) / K3$$

This amplifier is conditionally stable for given values of R1. As R1 is increased beyond 10 K $\Omega$ , it may become necessary to frequency compensate U1. This is done by placing a small capacitor from U1's output to its inverting input. This circuit uses 741 op-amps and will easily provide 100 KHz or greater bandwidth.

Figure 22. Unipolar photoconductive isolation amplifier

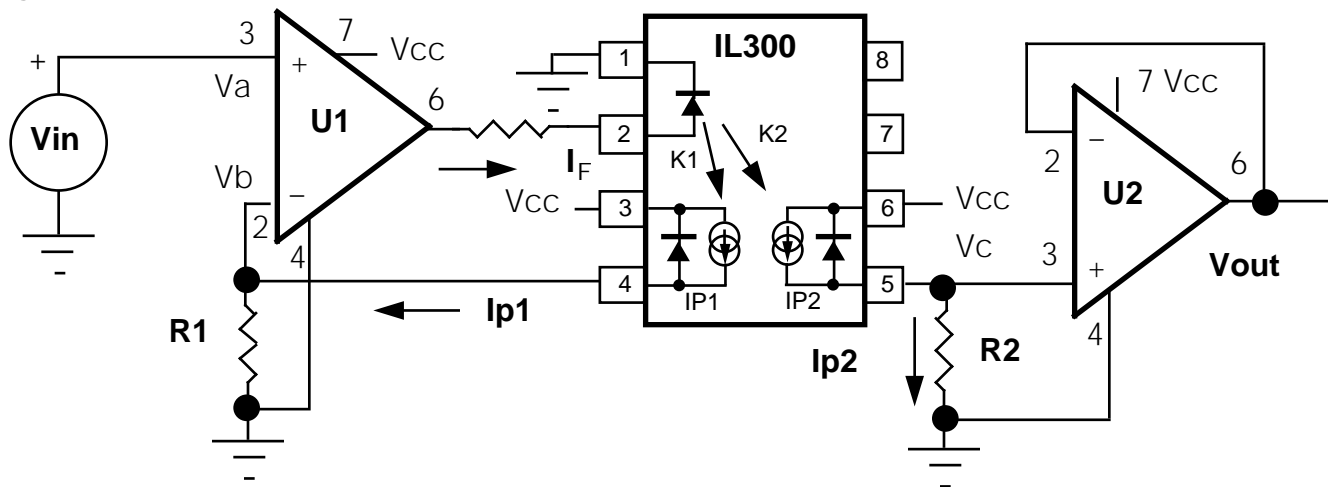
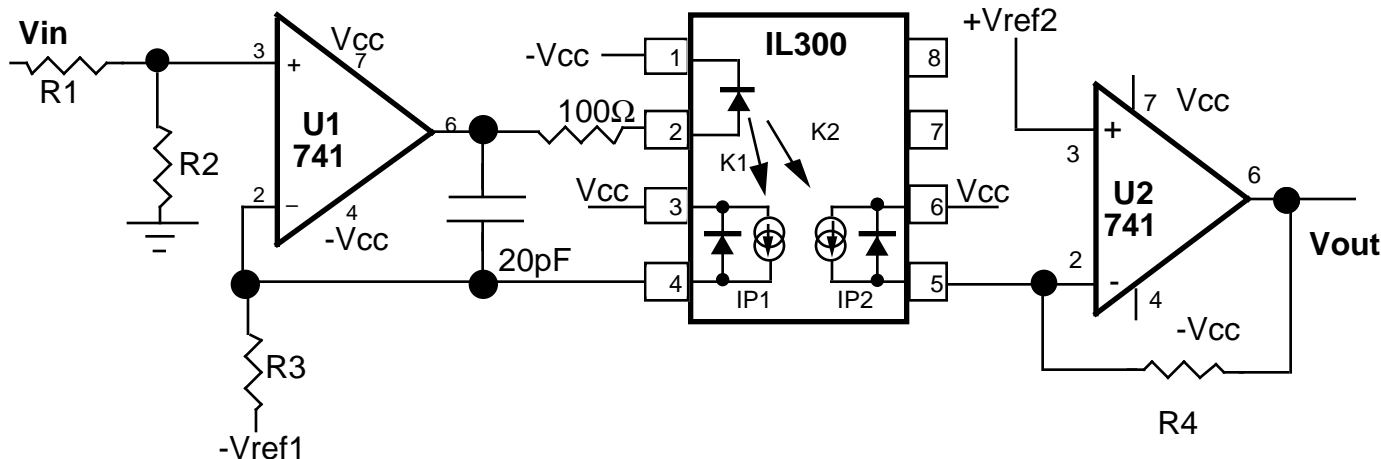


Figure 23. Bipolar photoconductive isolation amplifier



## Bipolar Isolation Amplifier

Many applications require the isolation amplifier to respond to bipolar signals. The generic inverting isolation amplifier shown in Figure 23 will satisfy this requirement. Bipolar signal operation is realized by prebiasing the servo loop. The prebias signal, Vref1, is applied to the inverting input through R3. U1 forces sufficient LED current to generate a voltage across R3 which satisfies U1's differential input requirements. The output amplifier, U2, is biased as a transresistance amplifier. The bias or offset, Vref2, is provided to compensate for bias introduced in the servo amplifier.

Much like the unipolar amplifier, selecting R3 is the first step in the design. The specific resistor value is set by the input voltage range, reference voltage, and the maximum output current,  $I_o$ , of the op-amp. This resistor value also affects the bandwidth and stability of the servo amplifier.

The input network of R1 and R2 form a voltage divider. U2 is configured as a inverting amplifier. This bipolar photoconductive isolation amplifier has a transfer gain given in Equation 30.

Equation 30:

$$\frac{V_{out}}{V_{in}} = \frac{K3 \cdot R4 \cdot R2}{R3 (R1 + R2)}$$

Equation 31 shows the relationship of the Vref1 to Vref2.

Equation 31:  $V_{ref2} = (V_{ref1} \cdot R4) / R3$

Another bipolar photoconductive isolation amplifier is shown in Figure 24. It is designed to accept an input signal of  $\pm 1$  V and uses inexpensive signal diodes as reference sources. The input signal is attenuated by 50% by a voltage divider formed with R1 and R2. The solution for R3 is given in Equation 30.

Equation 30:  $R3 = (0.5 \cdot V_{in_{max}} + V_{ref1}) / (I_F \cdot K1)$

For this design R3 equals 30 K $\Omega$ .

The output transresistance is selected to satisfy the gain requirement of the composite isolation amplifier. With  $K3 = 1$ , and a goal of unity transfer gain, the value of R4 is determined by Equation 33.

Equation 33:  $R4 = (R3 \cdot G \cdot (R1 + R2)) / (K3 \cdot R2)$   
 $R4 = 60 \text{ K}\Omega$

From Equation 31, Vref2 is shown to be twice Vref1. Vref2 is easily generated by using two 1N914 diodes in series.

This amplifier is simple and relatively stable. When better output voltage temperature stability is desired, consider the isolation amplifier configuration shown in Figure 25. This amplifier is very similar in circuit configuration except that the bias is provided by a high quality LM313 band gap reference source.

This circuit forms a unity gain non-inverting photoconductive isolation amplifier. Along with the LM113 references and low offset OP-07 amplifiers the circuit replaces the 741 opamps. A 2N2222 buffer transistor is used to increase the OP-07's LED drive capability. The gain stability is set by K3, and the output offset is set by the stability of OP-07s and the reference sources.

Figure 26 shows a novel circuit that minimizes much of the offset drift introduced by using two separate reference sources. This is accomplished by using an optically coupled tracking reference technique. The amplifier consists of two optically coupled signal paths. One IL300 couples the input to the output. The second IL300 couples a reference voltage generated on the output side to the input servo amplifier. This isolation amplifier uses dual opamps to minimize parts count. Figure 26 shows the output reference being supplied by a voltage divider connected to Vcc. The offset drift can be reduced by using a band gap reference source to replace the voltage divider.

Figure 24. Bipolar photoconductive isolation amplifier

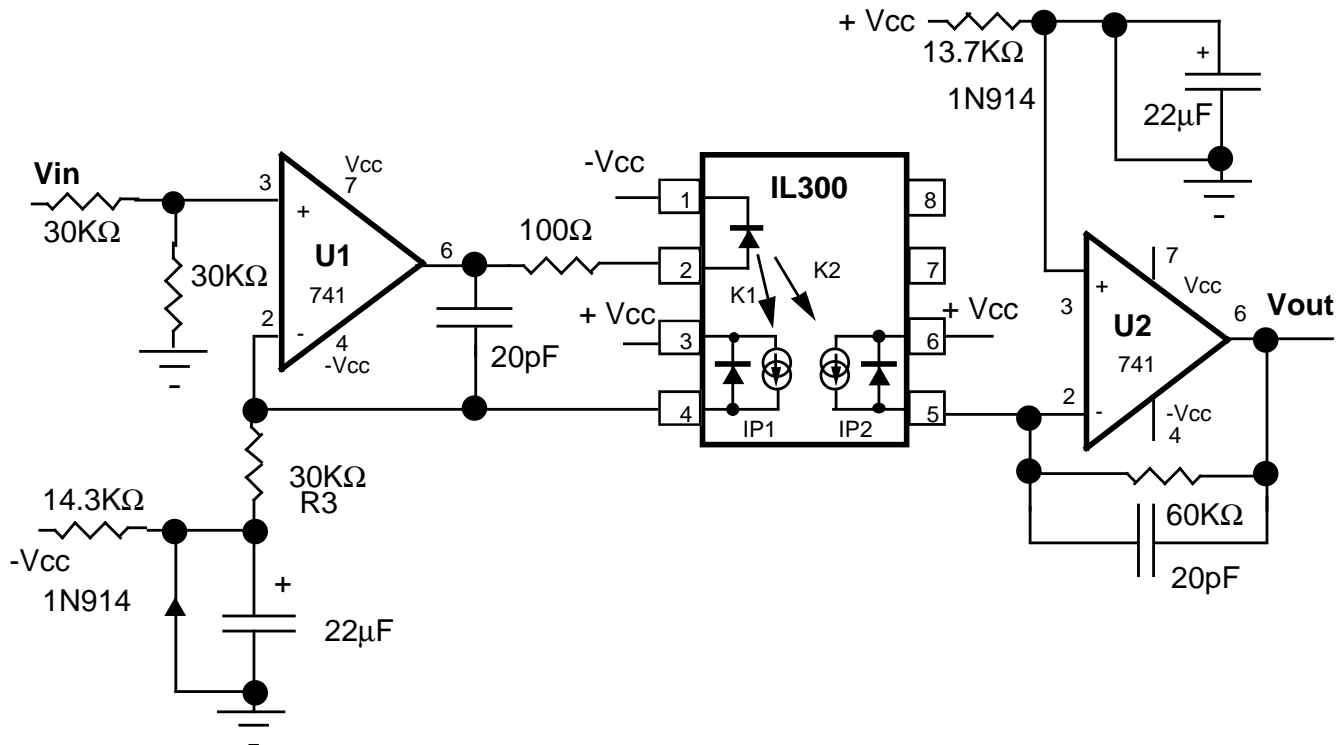


Figure 25. High stability bipolar photoconductive isolation amplifier

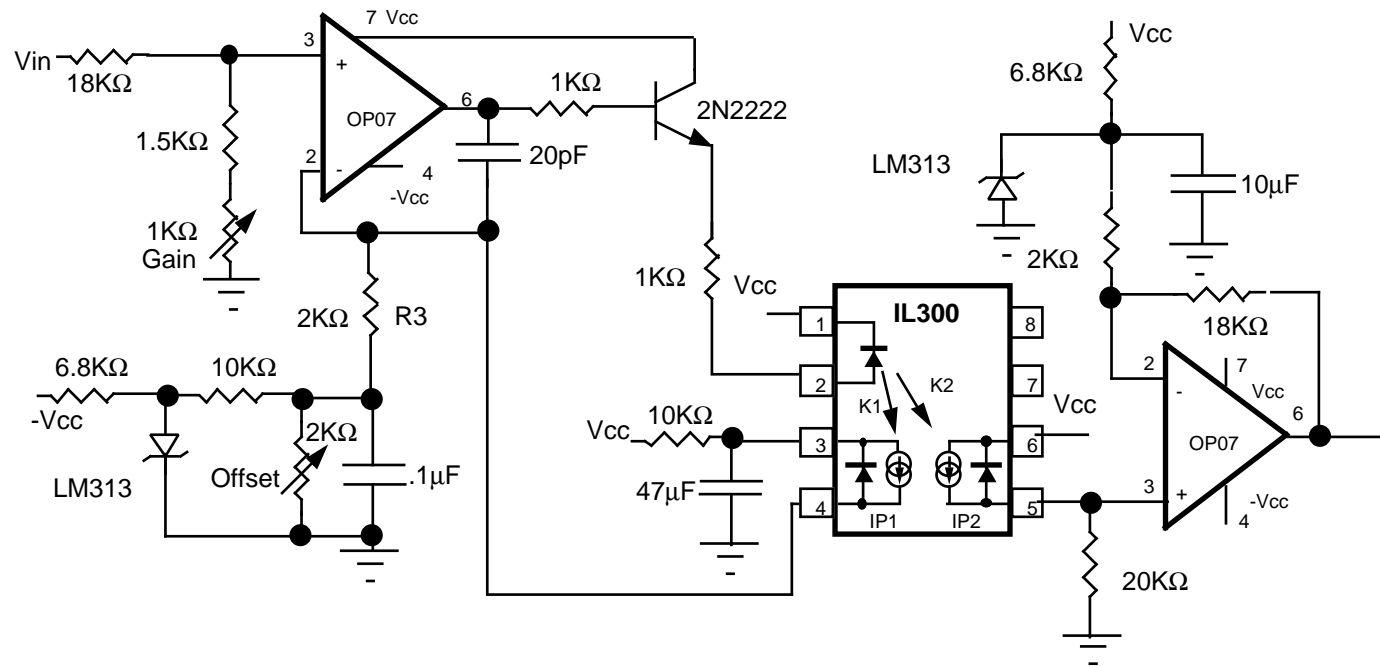
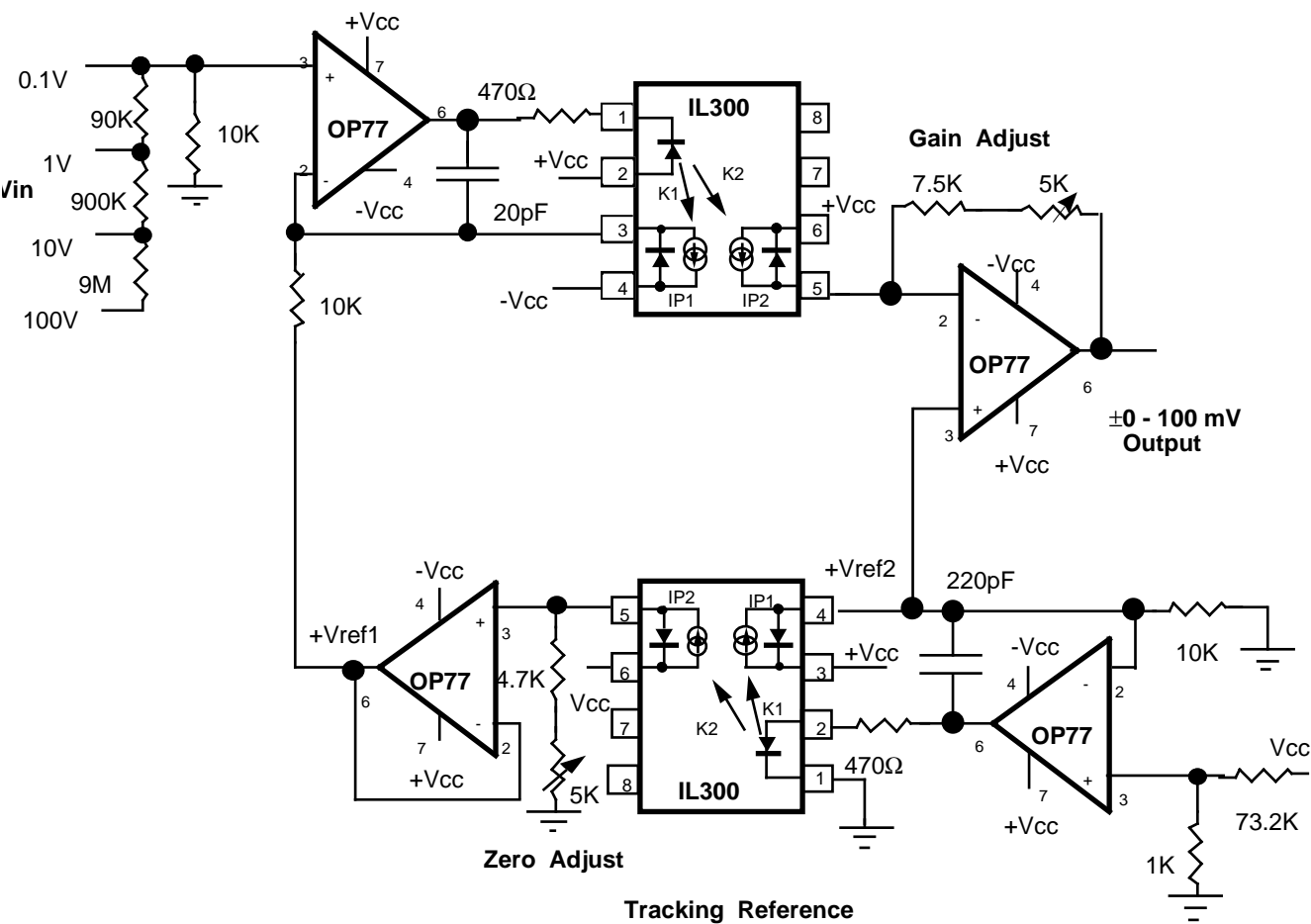


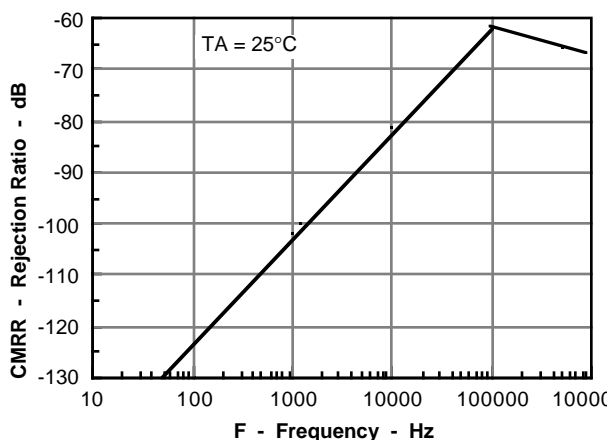
Figure 26. Bipolar photoconductive isolation amplifier with tracking reference



## Differential Photoconductive Isolation Amplifier

One of the principal reasons to use an isolation amplifier is to reject electrical noise. The circuits presented thus far are of a single ended design. The common mode rejection, CMRR, of these circuits is set by the CMRR of the coupler and the bandwidth of the output amplifier. The typical common mode rejection for the IL300 is shown in Figure 27.

**Figure 27. Common mode rejection**



The CMRR of the isolation amplifier can be greatly enhanced by using the CMRR of the output stage to its fullest extent. This

is accomplished by using a differential amplifier at the output that combines optically coupled differential signals. The circuit shown in Figure 28 illustrates the circuit.

Opamps U1 and U5 form a differential input network. U4 creates a 100  $\mu$ A,  $I_S$ , current sink which is shared by each of the servo amplifiers. This bias current is divided evenly between these two servo amplifiers when the input voltage is equal to zero. This division of current creates a differential signal at the output photodiodes of U2 and U6. The transfer gain,  $V_{out}/V_{in}$ , for this amplifier is given in Equation 34.

Equation 34:

$$\frac{V_{out}}{V_{in}} = \frac{R4 \cdot R2 \cdot K3(U5) + R3 \cdot R1 \cdot K3(U2)}{2 \cdot R1 \cdot R2}$$

The offset independent of the operational amplifiers is given in Equation 35.

Equation 35:

$$V_{offset} = \frac{I_S \cdot [R1 \cdot R3 \cdot K3(U2) - R2 \cdot R4 \cdot K3(U5)]}{R1 + R2}$$

Equation 35 shows that the resistors, when selected to produce equal differential gain, will minimize the offset voltage,  $V_{offset}$ . Figure 29 illustrates the voltage transfer characteristics of the prototype amplifier. The data indicates the offset at the output is -500  $\mu$ V when using 1 K $\Omega$  1% resistors.

**Figure 28. Differential photoconductive isolation amplifier**

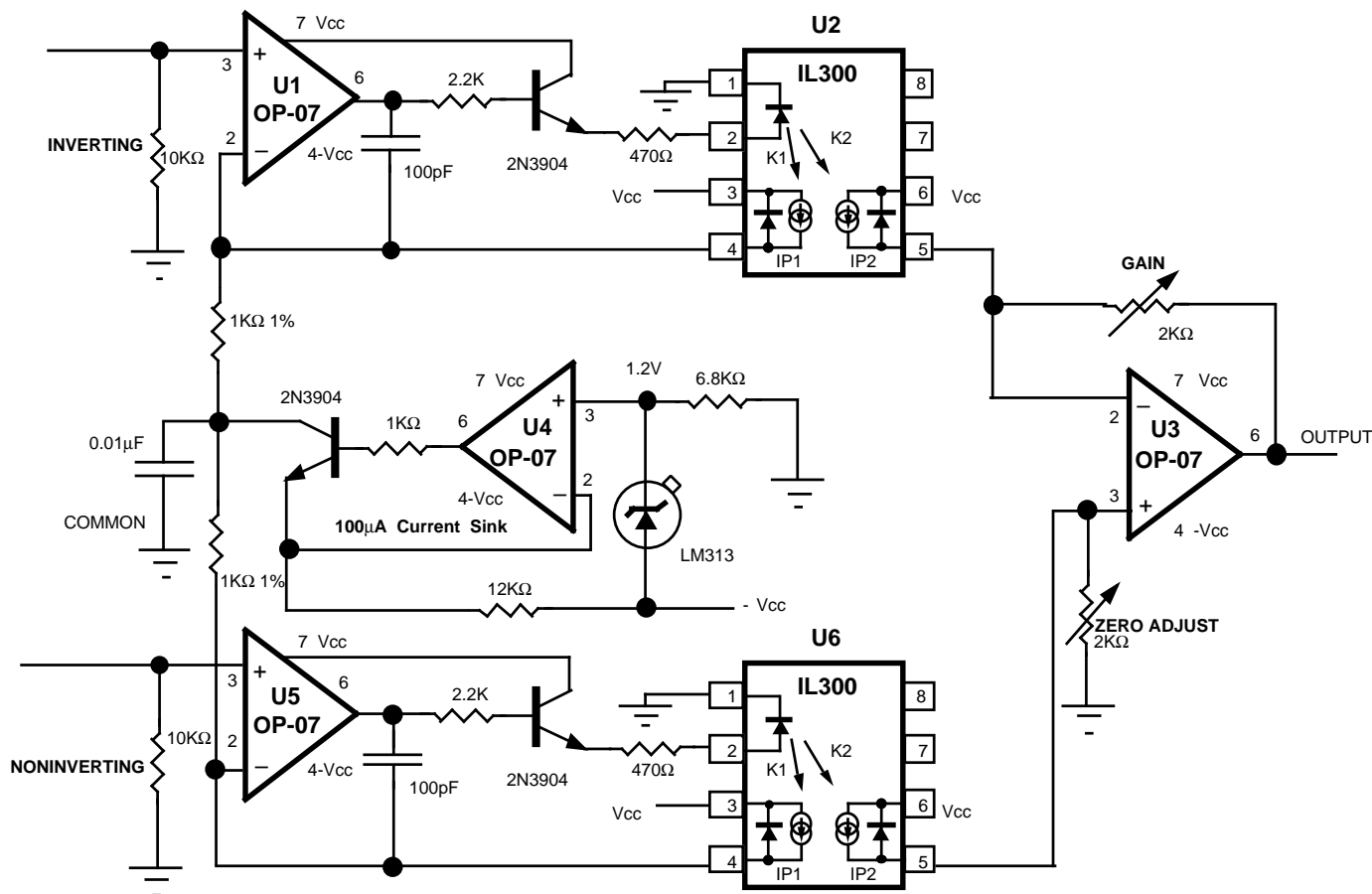


Figure 29. Differential photoconductive isolation amplifier transfer characteristics

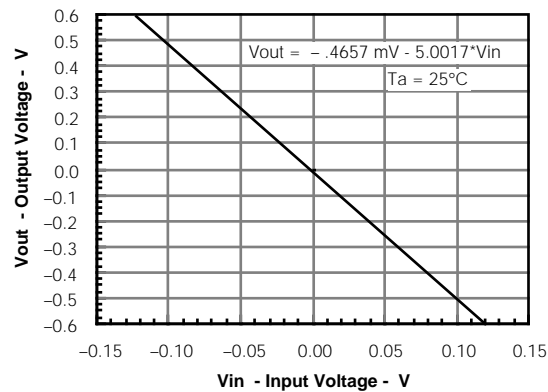
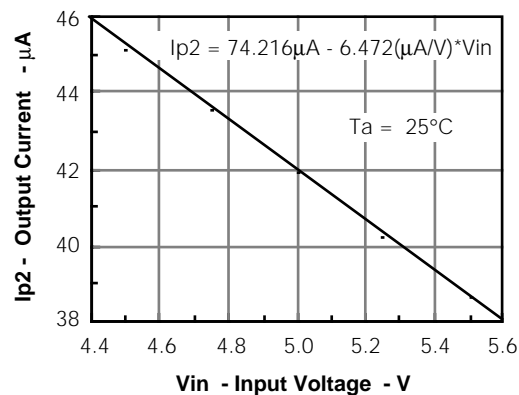


Figure 30. Transistor unipolar photoconductive isolation amplifier transfer characteristics



Discrete Isolation Amplifier

A unipolar photoconductive isolation amplifier can be constructed using two discrete transistors. Figure 32 shows such a circuit. The servo node, Va, sums the current from the photodiode and the input signal source. This control loop keeps Va constant. This amplifier was designed as a feedback control element for a DC power supply. The DC and AC transfer characteristics of this amplifier are shown in Figures 30 and 31.

Figure 32. Unipolar photoconductive isolation amplifier with discrete transistors

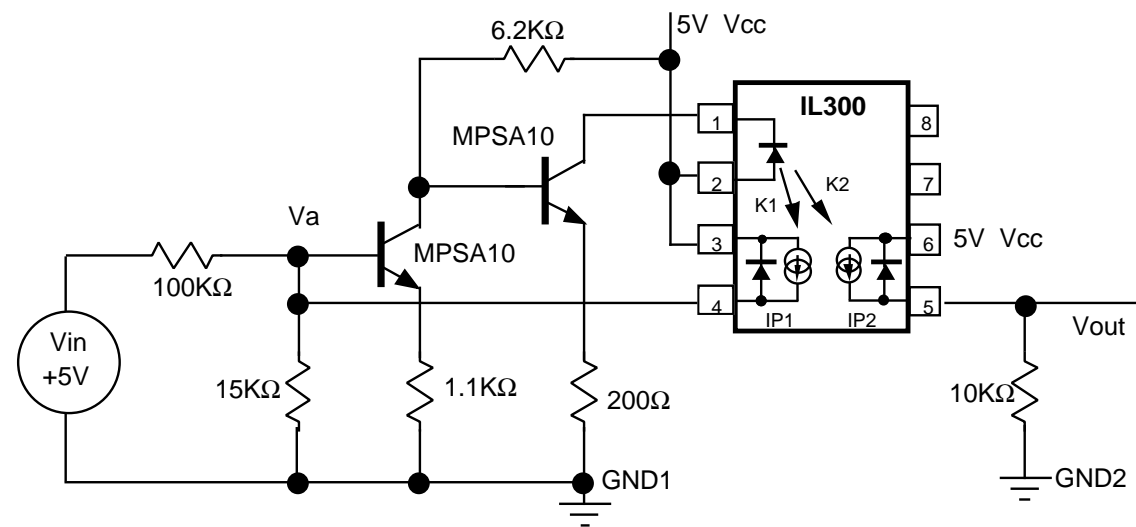
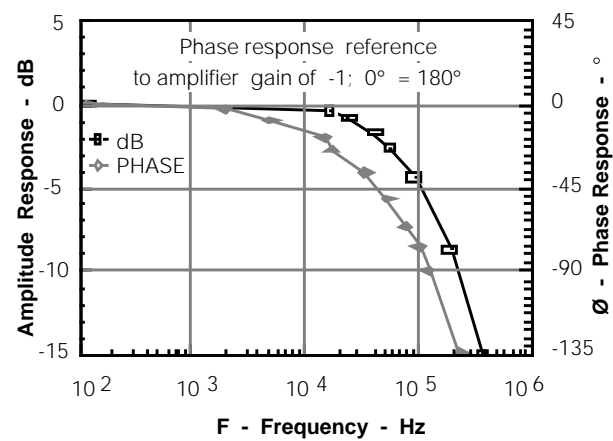


Figure 31. Transistor unipolar photoconductive isolation amplifier frequency and phase response



Conclusion

The analog design engineer now has a new circuit element that will make the design of isolation amplifiers easier. The preceding circuits and analysis illustrate the variety of isolation amplifiers that can be designed. As a guide, when highest stability of gain and offset is needed, consider the photovoltaic amplifier. Widest bandwidth is achieved with the photoconductive amplifier. Lastly, the overall performance of the isolation amplifier is greatly influenced by the operational amplifier selected. Noise and drift are directly dependent on the servo amplifier.

The IL300 also can be used in the digital environment. The pulse response of the IL300 is constant over time and temperature. In digital designs where LED degradation and pulse distortion can cause system failure, the IL300 will eliminate this failure mode.

## SUPPLEMENTAL INFORMATION

### Photodetector Operation Tutorial

#### Photodiode Operation and Characteristics

The photodiodes in the IL300 are PIN (P-material - Intrinsic material - N-material) diodes. These photodiodes convert the LED's incident optical flux into a photocurrent. The magnitude of the photocurrent is linearly proportional to the incident flux. The photocurrent is the product of the diode's responsivity,  $S_i$ , (A/W), the incident flux,  $E_e$  (W/mm<sup>2</sup>), and the detector area  $A_D$ , (mm<sup>2</sup>). This relationship is shown below:

$$\text{Equation 1a: } I_P = S_i \cdot E_e \cdot A_D$$

#### Photodiode I/V Characteristics

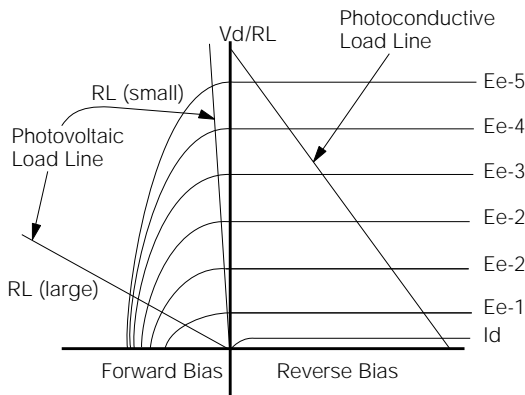
Reviewing the photodiode's current /voltage characteristics aids in understanding the operation of the photodiode, when connected to an external load. The I-V characteristics are shown in Figure 33. The graph shows that the photodiode will generate photocurrent in either forward biased (photovoltaic), or reversed biased (photoconductive) mode.

In the forward biased mode the device functions as a photovoltaic, voltage generator. If the device is connected to a small resistance, corresponding to the vertical load line, the current output is linear with increases in incident flux. As  $R_L$  increases, operation becomes nonlinear until the open circuit (load line horizontal) condition is obtained. At this point the open circuit voltage is proportional to the logarithm of the incident flux.

In the reverse biased (photoconductive mode), the photodiode generates a current that is linearly proportional to the incident flux. Figure 33 illustrates this point with the equally spaced current lines resulting from linear increase of  $E_e$ .

The photocurrent is converted to a voltage by the load resistor  $R_L$ . Figure 33 also shows that when the incident flux is zero ( $E_e=0$ ), a small leakage current, or dark current ( $I_D$ ) will flow.

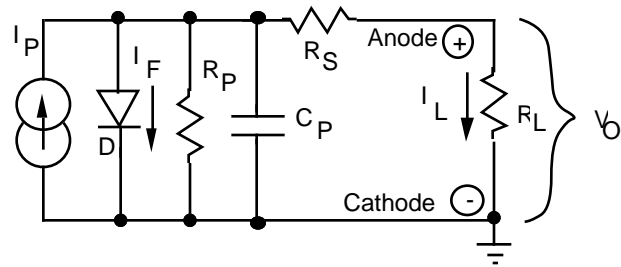
**Figure 33. Photodiode I/V characteristics**



#### Photovoltaic Operation

Photodiodes, operated in the photovoltaic mode, generate a load voltage determined by the load resistor,  $R_L$ , and the photocurrent,  $I_P$ . The equivalent circuit for the photovoltaic operation is shown in Figure 34. The photodiode includes a current source ( $I_P$ ), a shunt diode (D), a shunt resistor ( $R_P$ ), a series resistor ( $R_S$ ), and a parallel capacitor ( $C_P$ ). The intrinsic region of the PIN diode offers a high shunt resistance resulting in a low dark current, and reverse leakage current.

**Figure 34. Equivalent circuit--photovoltaic mode**

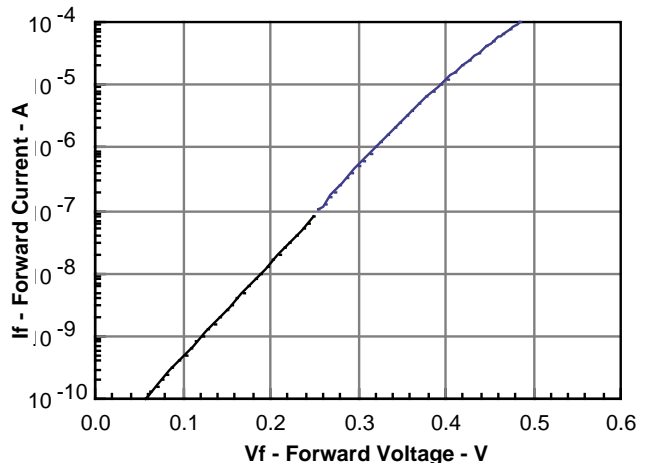


The output voltage,  $V_0$ , can be determined through nodal analysis. The circuit contains two nodes. The first node,  $V_F$ , includes the photocurrent generator,  $I_P$ , the shunt diode, D, shunt resistor ( $R_P$ ), and parallel capacitance,  $C_P$ . The second node,  $V_O$ , includes: the series resistor,  $R_S$ , and the load resistor,  $R_L$ . The diode, D, in the  $V_F$  node is responsible for the circuit's nonlinearity. The diode's current voltage relationship is given in Equation 2a.

$$\text{Equation 2a: } I_F = I_S \cdot [\text{EXP}(V_F / K) - 1]$$

This graphical solution of 2a for the IL300 is shown in Figure 35.

**Figure 35. Photodiode forward voltage vs. forward current**



Inserting the diode Equation 2a, into the two nodal equations gives the following DC solution for the photovoltaic operation (Equation 3a):

$$\text{Equation 3a}$$

$$0 = I_P - I_S \cdot \{\text{EXP}[V_O \cdot (R_S + R_L) / K \cdot R_L] - 1\} - V_O \cdot [(R_S + R_L + R_P) / R_P \cdot R_L]$$

Typical IL300 values:

$$I_S = 13.94 \cdot 10^{-12}$$

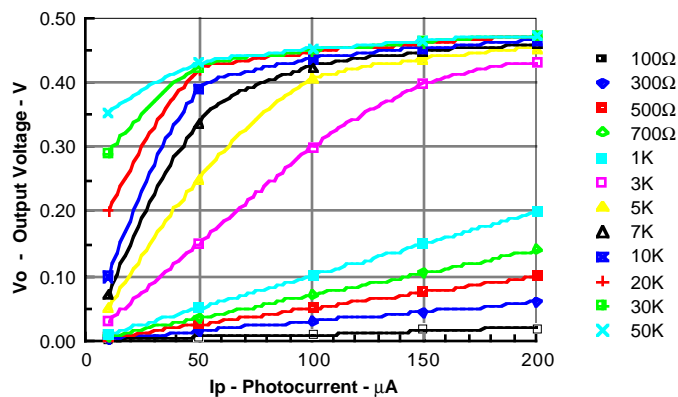
$$R_S = 50 \Omega$$

$$R_P = 15 \text{ G}\Omega$$

$$K = 0.0288$$

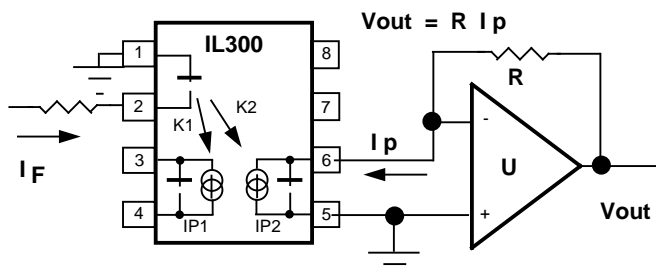
By inspection, as  $R_L$  approaches zero ohms the diode voltage,  $V_F$ , also drops. This indicates a small diode current. All of the photocurrent will flow through the diode series resistor and the external load resistor. Equation 3a was solved with a computer program designed to deal with nonlinear transcendental equations. Figure 36 illustrates the solution.

**Figure 36. Photovoltaic output vs. load resistance and photocurrent**



This curve shows a series of load lines, and the output voltage,  $V_o$ , caused by the photocurrent. Optimum linearity is obtained when the load is zero ohms. Reasonable linearity is obtained with load resistors up to 1000 ohms. For load resistances greater than 1000  $\Omega$ , the output voltage will respond logarithmically to the photocurrent. This response is due to the nonlinear characteristics of the intrinsic diode,  $D$ . Photovoltaic operation with a zero ohm load resistor offers the best linearity and the lowest dark current,  $I_D$ . This operating mode also results in the lowest circuit noise. A zero load resistance can be created by connecting the photodiode between the inverting and non-inverting input of a transresistance operational amplifier, as shown in Figure 37.

**Figure 37. Photovoltaic amplifier configuration**



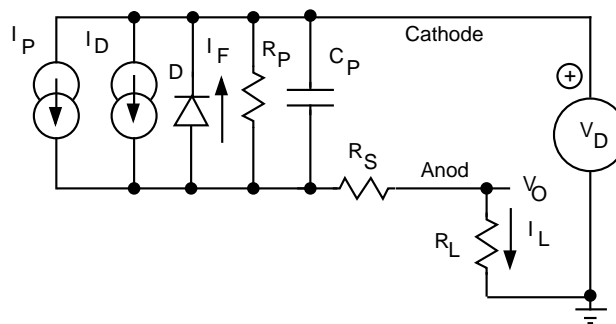
### Photoconductive Operation Mode

Isolation amplifier circuit architectures often load the photodiode with resistance greater than zero ohms. With non-zero loads, the best linearity is obtained by using the photodiode in the photoconductive or reverse bias mode. Figure 38 shows the photodiode operating in the photoconductive mode. The output voltage,  $V_o$ , is the product of the photocurrent times the load resistor.

The reverse bias voltage causes a small leakage or dark current,  $I_D$ , to flow through the diode. The output photocurrent and the dark current, sum the load resistor. This shown in Equation 4a.

$$\text{Equation 4a: } V_L = R_L \cdot (I_P + I_D)$$

**Figure 38. Photoconductive photodiode model**



The dark current depends on the diode construction, reverse bias voltage and junction temperature. The dark current can double every 10°C. The IL300 uses matched PIN photodiodes that offer extremely small dark currents, typically a few picoamps. The dark current will usually track one another, and their effect will cancel each other when a servo amplifier architecture is used. The typical dark current as a function of temperature and reverse voltage is shown in Figure 39.

The responsivity,  $S$ , of the photodiode is influenced by the potential of the reverse bias voltage. Figure 40 shows the responsivity percentage change versus bias voltage. This graph is normalized to the performance at a reverse bias of 15 volts. The responsivity is reduced by 4% when the bias is reduced to 5 volts.

**Figure 39. Dark current vs. reverse bias**

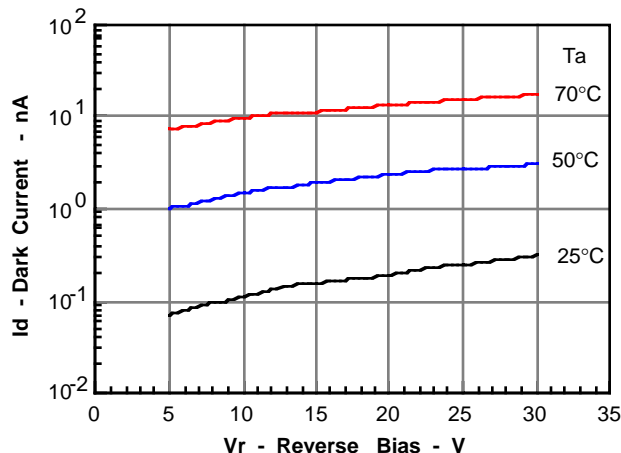
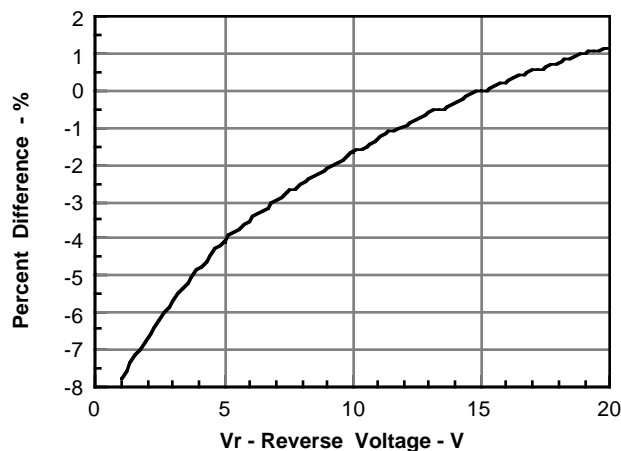


**Figure 40. Photoconductive responsivity vs. bias voltage**





The photodiode operated in the photoconductive mode is easily connected to an operational amplifier. Figure 41 shows the diode connected to a transresistance amplifier. The transfer function of this circuit is given in Equation 5a.

$$\text{Equation 5a: } V_{\text{out}} = R \cdot (I_P + I_d)$$

#### Bandwidth Considerations

PIN photodiodes can respond very quickly to changes in incident flux. The IL300 detectors respond in tens of nanoseconds. The slew rate of the output current is related to the diodes junction capacitance,  $C_j$ , and the load resistor,  $R$ . The product of these two elements set the photo-response time constant.

$$\text{Equation 6a: } \tau = R \cdot C_j$$

This time constant can be minimized by reducing the load resistor,  $R$ , or the photodiode capacitance. This capacitance is reduced by depleting the photodiode's intrinsic region,  $I$ , by applying a reverse bias. Figure 42 illustrates the effect of photodiode reverse bias on junction capacitance.

**Figure 41. Photoconductive amplifier**

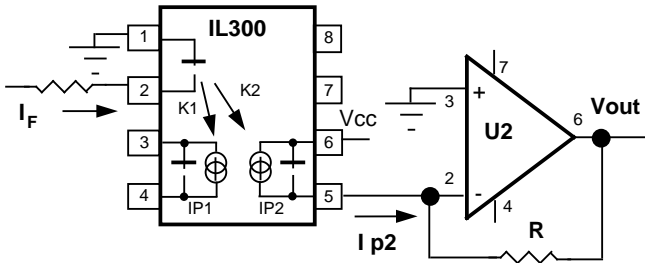
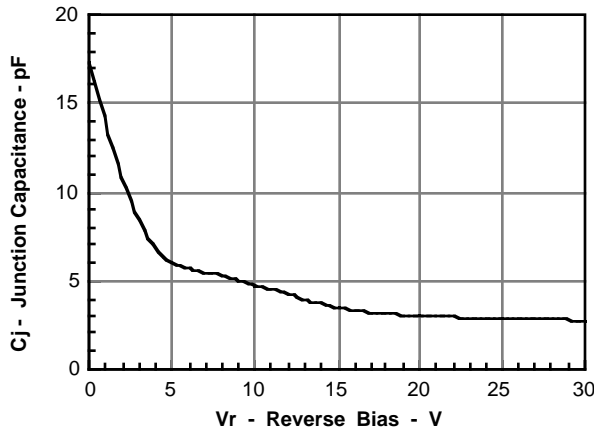


**Figure 42. Photodiode junction capacitance vs. reverse voltage**



The zero biased photovoltaic amplifier offers a 50 KHz-60 KHz usable bandwidth. When the detector is reverse biased to -15 V, the typical isolation amplifier response increases to 100-150 KHz. The phase and frequency response for the IL300 is presented in Figure 43. When maximum system bandwidth is desired, the reverse biased photoconductive amplifier configuration should be considered.

**Figure 43. Phase and frequency response**

